**Natural Hazards
and Earth
System Sciences**

Spectral and multifractal study of electroseismic time series associated to the M_w=6.5 earthquake of 24 October 1993 in Mexico

A. Ramírez-Rojas[1], A. Muñoz-Diosdado[2], C. G. Pavía-Miller[1, 3], and F. Angulo-Brown[3]

[1]Área de Física de Procesos Irreversibles, Departamento de Ciencias Básicas, Universidad Autónoma Metropolitana Azcapotzalco, 02200, México D. F., México
[2]Departameno de Matemáticas, Unidad Profesional Interdisciplinaria de Biotecnología, Instituto Politécnico Nacional, 07340, México D. F., México
[3]Departamento de Física, Escuela Superior de Física y Matemáticas, Instituto Politécnico Nacional, Edif. Nº 9, U. P. Zacatenco, 07738, México D.F., México

Abstract. In this work we present a spectral and multifractal study of the electric self-potential fluctuations registered in an electroseismic station located at 100 km from the epicenter of an earthquake (EQ) with M_w=6.5 in the Pacific coast of Mexico. Our study suggests that in general the time series analyzed displays a persistent behavior. Our results show an anticorrelation between the spectral exponent β and the width of the multifractal spectrum $\Delta\alpha$, when they are calculated during a time interval of five months (four months before the EQ and one month after the EQ). In addition, we also calculate the time evolution of the correlation coefficient finding that it has a very similar behavior that the time evolution of $\Delta\alpha$.

1 Introduction

In some recent papers fractal methods have been applied in order to extract possible earthquake precursory signatures from scaling properties of both ULF geomagnetic data (Hayakawa et al., 1999; Smirnova et al., 2001; Telesca et al., 2001; Gotoh et al., 2003), and electric seismic signals (Ramírez-Rojas et al., 2004; Varotsos et al., 2002, 2003a; Kapiris et al., 2003, 2004). It has been found that the power spectrum of ULF emissions, on average exhibits a power law behavior $S(f)\sim f^{-\beta}$, which is a fingerprint of typical fractal (self-affine) time series. In most of the cases, the spectral exponent β displays a tendency to decrease gradually when approaching the earthquake date. Such a tendency shows a gradual evolution of the structure of the ULF noise towards a typical flicker noise structure ($1/f$ noise-like) in the proximity of a large earthquake. This behavior has been sug-

gested as an earthquake precursory signature (Hayakawa et al., 1999; Smirnova et al., 2001; Ramírez-Rojas et al., 2004).

In the present work we analyze the M_w=6.5 earthquake occurred at the coordinates (16.54° N, 98.98° W) on the South Pacific Mexican coast on 24 October 1993. The electroseismic dataset was collected at the Acapulco station located 100 km far away from the epicenter. Our work is focused on showing that the observed behavior of the spectral exponent β_1 (the spectral exponent for low frequency intervals, see below), describes a remarkable decreasing a month and a half before the event date approximately, just as it was observed in other events (Hayakawa et al., 1999; Smirnova et al., 2001; Telesca et al., 2001; Ramírez-Rojas et al., 2004 in the EW channel). It is convenient to remark that our approach is not focused in the search of individual SES features with a precise duration in the sense of Varotsos et al. (2002, 2003a) and Kapiris et al. (2004), but in the analysis of the global time series considered. On the other hand, we suggest an anticorrelation relationship between both the time evolution of β_1 and the width of the multifractal spectra $\Delta\alpha$ of the electroseismic files corresponding to the time interval studied. The paper is organized as follows: in Sect. 2, we present the analyzed data sets and a resume of the methods used for the corresponding analysis. In Sect. 3 we discuss our results and finally we present some concluding remarks.

2 Data and analysis tools

The seismic electric registers, $V(t)$, were obtained as the fluctuations of the electric self-potential monitored directly from the ground by means of two dipoles oriented in North-South direction (NS channel) and the other one in East-West direction (EW channel). The electrodes were buried 2 m into the ground with a separation between them of L=50 m. The signals that we consider for this study were collected from
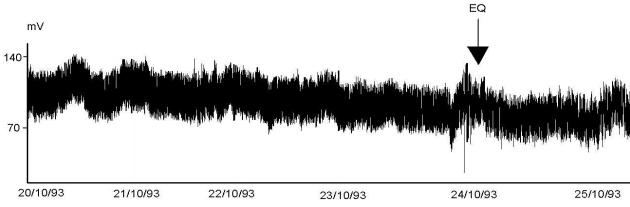
Fig. 1. Six days segment of the NS time series. The arrow indicates the EQ date.

the NS channel and monitored with two sampling rates, (first at $\Delta t=4$ s and then $\Delta t=2$ s) in different time intervals. A low pass filter was used in order to get signals filtered in the ULF range, $0 < f < 0.125$ Hz, for more technical details, Yépez et al. (1995) is recommended. In Fig. 1 we show a six days segment of the time series $V(t)$ in the NS channel.

Power spectral density is a well-established method to investigate the temporal fluctuations of a time series. The power spectrum is defined (Turcotte, 1992) as:

$$S(f) = \lim_{T \to \infty} \left\{ \frac{|X(f,T)|^2}{T} \right\}. \tag{1}$$

Here, $X(f,T)$ is the Fourier Transform of the time series $V(t)$, T is the total time of monitoring with $T=n\Delta t$, where Δt is the sampling rate.

For self-affine time series, the power spectrum behaves like a power-law relation with frequency given by, $S(f) \sim f^{-\beta}$. First, $S(f)$ is calculated by means of the Fast Fourier Transform (FFT) algorithm, and the spectral exponent β is estimated by the slope of the best-fit straight line to $\log(S(f))$ vs. $\log(f)$ and, according with Malamud and Turcotte (2001), β characterizes the temporal fluctuations of the time series, for example a white noise-type has $\beta=0$, for a flicker noise or $1/f$ noise, $\beta=1$, and for the Brownian motion $\beta=2$.

The method of Detrended Fluctuation Analysis (DFA) (Peng et al., 1994) has proven to be useful in revealing the extent of long-range correlations and has some advantages over conventional methods because it permits the detection of intrinsic self-similarity embedded in a seemingly nonstationary time series (Varotsos et al., 2002). The method is described briefly: The time series to be analyzed is first integrated. Next, the integrated time series is divided into boxes of equal length, n. In each box of length n, a least squares line (or polynomial curve of order k) is fitted to the data (representing the trend in that box). Next, we detrend the integrated time series by subtracting the local trend in each box. The root-mean-square fluctuation of this integrated and detrended time series is calculated and denoted as $F(n)$. This computation is repeated over all time scales (box sizes), from $n =$ minbox to $n =$ maxbox, to characterize the relationship between $F(n)$, the average fluctuation, and n, the box size. Typically, $F(n)$ will increase with the box size n. A linear re-

lationship in a log-log plot indicates the presence of a power law (fractal) scaling:

$$F(n) \propto n^{\gamma}. \tag{2}$$

Under such conditions, the fluctuations can be characterized by the scaling γ-exponent, i.e. the slope of the line relating $\log((F(n))$ to $\log(n)$. The case $\gamma=1/2$ represents the absence of long-range correlations. Thus, the double logarithmic plot revels the presence or not, of long-range correlations ($\gamma \neq 1/2$).

The behavior of nonlinear dynamical systems can be often characterized by fractal or multifractal measures. Monofractals can be characterized by a single fractal dimension, which indicates that they are stationary from the viewpoint of their local scaling properties. Multifractals can be decomposed into many subsets characterized by different fractal dimensions. Multifractals have been used for example to describe turbulent flows (Chhabra et al., 1989), to identify pathological conditions in heartbeat dynamics (Ivanov et al., 1999), to show an underlying hierarchical structure in proteins (Balafas and Dewey, 1995) or to reproduce many important stylized facts of speculative markets (Yamasaki and Mackin, 2003). Various multifractal formalisms have been developed to describe the statistical properties of these measures in terms of their singularity spectrum, which provides a description of the multifractal measure in terms of interwoven sets, with singularity strength α (the Lipschitz-Hölder exponent), whose fractal dimension is $f(\alpha)$ (Feder, 1988; Chhabra et al., 1989). We use the Chhabra and Jensen algorithm for the calculation of the spectrum of multifractal structures because it has been reported (Chhabra and Jensen, 1989; Chhabra et al., 1989) that this method provides a highly accurate, practical and efficient method for direct computation of the singularity spectrum.

If we cover the support of the measure with boxes of size L and define $P_i(L)$ as the probability in the *ith* box, then we can define an exponent α by

$$P_i(L) \approx L^{\alpha_i} \tag{3}$$

and if we count the number of boxes $N(\alpha)$ where the probability $P_i(L)$ has a singularity strength between α and $\alpha+d\alpha$, the $f(\alpha)$ can be defined as the fractal dimension of the set of boxes with singularity strength α by

$$N(\alpha) \approx L^{-f(\alpha)}. \tag{4}$$

First, a 1-parameter manifold of normalized measures $\mu_i(q)$ is constructed, where the probabilities in the boxes of size L are

$$\mu_i(q,L) = \frac{[P_i(L)]^q}{\sum_j [P_j(L)]^q}. \tag{5}$$

Finally, for each value of q we evaluate the numerators on the right-hand sides of the equations:

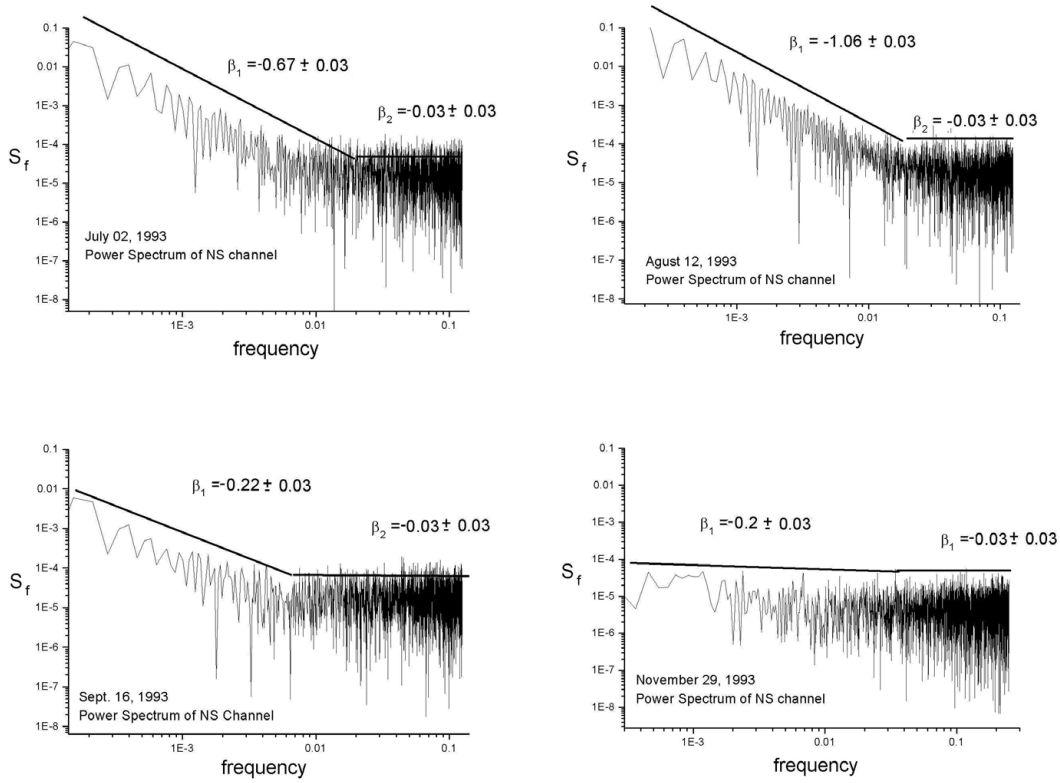$$f(q) = \lim_{L \to 0} \frac{\sum_i \mu_i(q,L) \ln[\mu_i(q,L)]}{\ln L} \tag{6}$$

Fig. 2. Here we show four cases representing the typical power spectrum behavior of our time series. They exhibit a crossover between two different β's.

$$\alpha(q) = \lim_{L \to 0} \frac{\sum_i \mu_i(q, L) \ln[P_i(L)]}{\ln L} \qquad (7)$$

for decreasing box sizes (increasing n), and we extract $f(q)$ and $\alpha(q)$ from the slopes of the numerators versus $\ln L$ ($f(q)$ and $\alpha(q)$ are obtained applying the least squares method). The parameter q provides a microscope for exploring different regions of the singular measure. For $q>1$, $\mu(q)$ amplifies the more singular regions of P, while for $q<1$ it accentuates the less singular regions, and for $q=1$ the measure μ (Eq. 5) replicates the original measure.

These equations provide a relationship between the fractal dimension f and the average singularity strength α as implicit functions of the parameter q.

3 Results and discussion

In order to analyze the whole time series monitored from July up to November 1993, a sequence of 6 h-files segments was chosen. The power spectrum $S(f)$ was performed for each segment by using a FFT algorithm, then the corresponding β exponent was estimated as the best fit slope in a log-log scale of the power law relation $S(f) \sim f^{-\beta}$ (which is a characteristic feature of fractal time series). We found that $S(f)$ shows two exponents, one of them β_1, for low frequencies ($0 < f < 0.01$ Hz), and a β_2 exponent for high frequencies
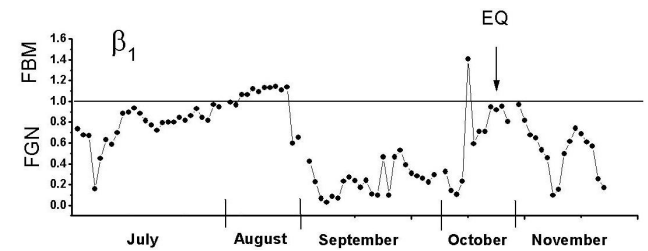

Fig. 3. Time evolution of β_1. It is remarkable that in general $0 < \beta_1 \leq 1$ that is in the FGN range, with a persistence behavior. Only a few β_1-values are over the $\beta_1 = 1$ line.

($0.01 < f < 0.125$ Hz). We always observed that practically $\beta_2 \approx 0$ with a white noise-like behavior (see Fig. 2).

The dynamical evolution of β_1 was analyzed from July until November 1993, in this period a $M_w = 6.5$ earthquake occurred on 24 October. In general, we observed that the emission spectrum displays a power law-like behavior $S(f) \sim f^{-\beta_1}$ for low frequencies. Figure 3 shows the dynamics followed by β_1. Three time intervals with different kind of behavior can be distinguished, these intervals were heuristically chosen and are different to the epochs used by Kapiris et al. (2004). The first interval starts at the beginning of July and finishes at almost the end of August, where β_1 describes an increasing quasi linear trend in the range of $0.55 < \beta_1 < 1.1$ approximately.
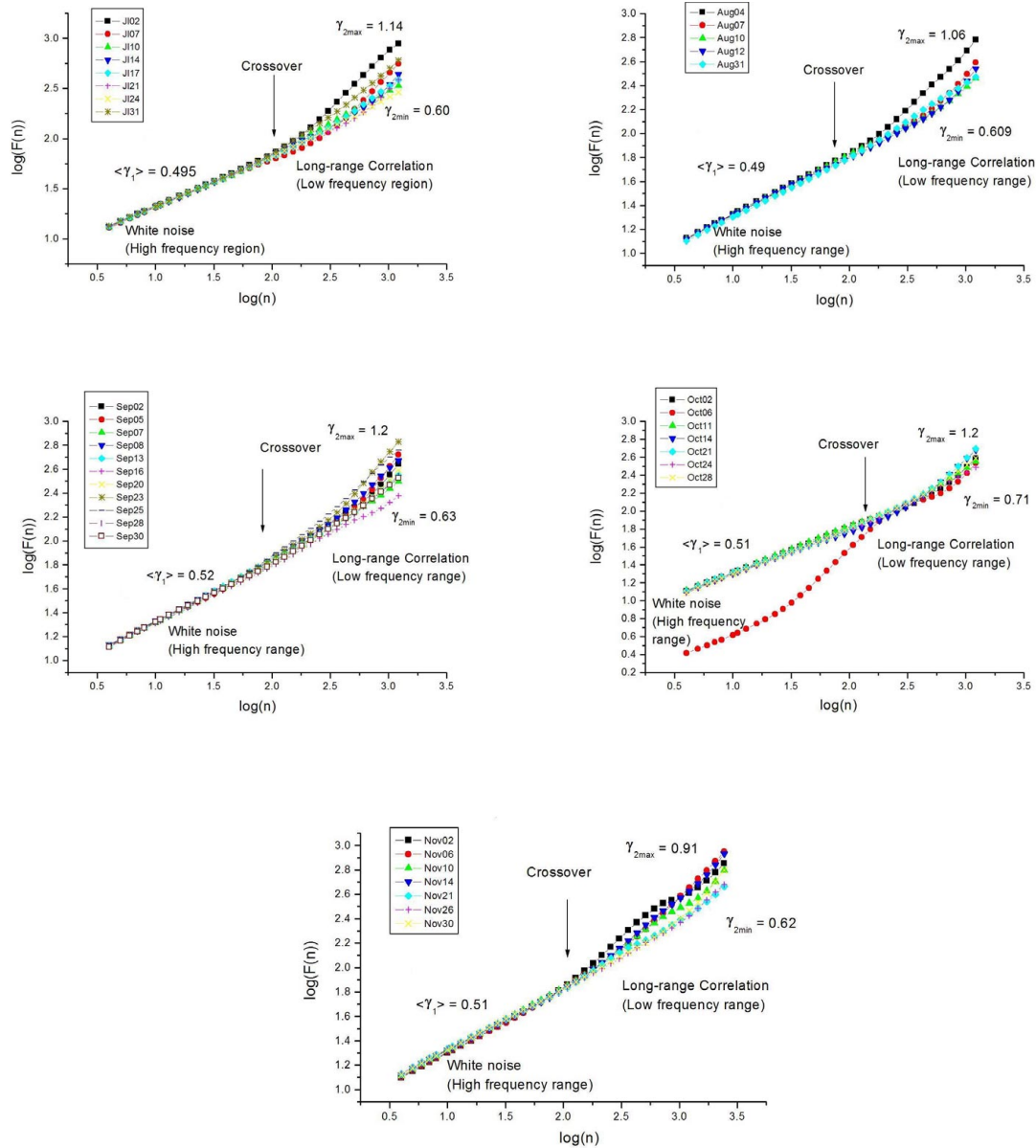
Fig. 4. DFA performed on some 6 h files of each month. It can be observed that the complete time series exhibits two mixed processes. For the high frequency range the process is dominated by a white noise. For the low frequency range, the dynamics represents mainly a long-range correlated mechanism.

The second interval corresponds to a period where suddenly β_1 falls by taking values in the range, $0 < \beta_1 < 0.55$. This behavior is observed from the end of August until the first week of October. The third interval occurs from October to November. The slope β_1 describes large fluctuations during a pair of weeks before the quake, and some days around the EQ, β_1 achieves values of the order of 0.8 in average. At the end of October and at the beginning of November, β_1 shows a decreasing behavior. The arrow marks the date of the M_w=6.5 quake. In our analysis we found that β_1 runs in the interval (0.55, 1.2) from July to August (Fig. 3), this region approximately corresponds to a fractional Gaussian noise (FGN) (Heneghan and McDarby, 2000). The trend maintained by β_1 suddenly decreases until

the range $0 < \beta_1 < 0.55$. Finally, two weeks before the quake, β_1 grows obtaining their largest value ($\sim$1.7). Our β_1-values are in general (with a few exceptions) within a persistence interval with Hurst exponents H in the interval $0.5 < H < 1$ according with the expression $H = (\beta + 1)/2$ for FGN (Heneghan and McDarby, 2000). It is important to remark that our time series surely are contaminated by artificial man-made noises (and other natural noises) and our analysis does not distinguish between true seismic signals and artificial noises. In fact our study is over the global time series embedding possible signals with seismic origins and others of several causes. Interestingly, nevertheless the great noisy contamination of our time series, some long-range correlations arise.
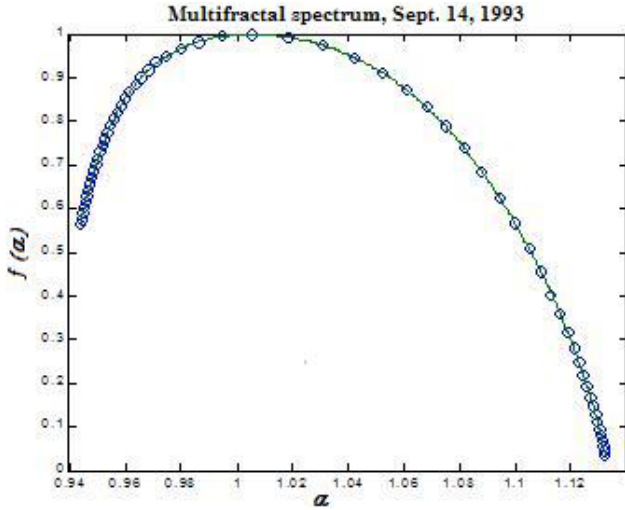
Fig. 5. Multifractal spectrum plot for the sequence of the 14 September six-hour segment.

Fig. 6. The width of the multifractal spectra versus time. Time series monitored from July to November 1993.

The Detrended Fluctuations Analysis (DFA) has been performed over several segments in order to reveal or not the presence of long-range correlations, that is: $\gamma=0.5$ indicates completely uncorrelated or white noise; $\gamma=1.0$ indicates $1/f$ noise; $\gamma=1.5$ indicates Brown noise and $0.5<\gamma<1.0$ indicates long-range correlations (Peng et al., 1994). In Fig. 4 five situations are showed. All of the cases exhibit a crossover indicating two overlapping processes. For high frequencies $(0<\log(n)<2.5)$ as we said before the process is approximately a white noise with $\gamma\sim0.5$. For low frequencies $(\log(n)>2.5)$, γ is in the interval $0.6<\gamma<1.2$ (with only a few cases where $\gamma>1$), that is, a process corresponding to long-range correlations. A crossover in the DFA exponent has been also reported by Varotsos et al. (2002) for SES activity. Although, we are not identifying particular SES activity our DFA exponents also present a crossover behavior with the properties aforementioned. In our case for high frequencies we observe a white noise type behavior while Varotsos et al. (2002) reported a $\gamma\approx0.88$. However for low frequencies our γ-values are of the same order as those of Varotsos et al. (2002) γ-values. Apparently in our noisy signals the environmental white noise remains present in the high frequencies intervals, nevertheless in the low-frequencies interval, long-range correlations arise. It is remarkable that in the Varotsos et al. (2002) SES activity, all the interval is dominated by long-range correlations.

The f versus α curves are the multifractal spectra, they have the appearance we show in Fig. 5. The spectra were calculated from $q=-30$ to $q=30$, after the algorithm was applied to the time series we smoothed the curves using cubic splines and extrapolated to obtain α_{max} and α_{min}. The spectrum width or degree of multifractality is defined as $\Delta\alpha=\alpha_{max}-\alpha_{min}$.

When we plot $\Delta\alpha$ versus time, we obtain the graphic of Fig. 6. In this figure we observe certain kind of anti-correlation between the width of the multifractal spectrum
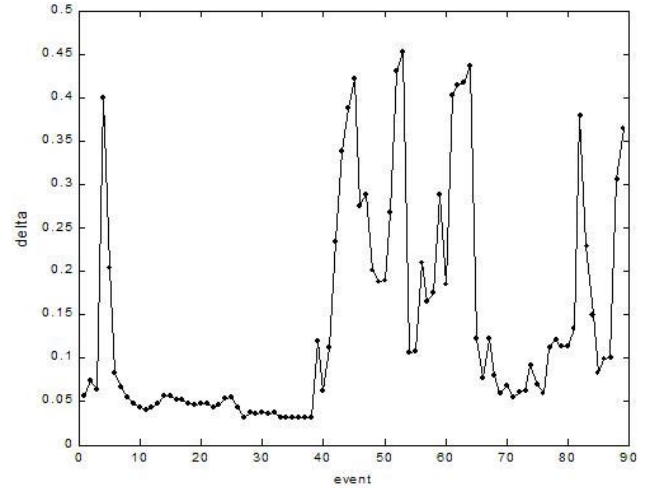
and the β_1 exponent (Fig. 3). During months of July and August $\Delta\alpha$ was very small practically every day, almost indicating a monofractal behavior, but the values of this width in September were abnormally high, indicating almost a transition toward a multifractal behavior one month previous the EQ.

We calculated the anti-correlation between $\Delta\alpha$ and β_1 for the interval July–November and we obtained the following relation:

$$\Delta\alpha = 0.3396 - 0.3260\beta_1 \qquad (8)$$

with a correlation coefficient $R=-0.699$, it looks approximately as

$$\Delta\alpha = \frac{1}{3}(1 - \beta_1) \qquad (9)$$

that is an empirical relation between $\Delta\alpha$ and β_1, and apparently it only is valid for $0<\beta_1\leq1$, that is within the FGN range.

We used it to calculate the curve $\Delta\alpha$ versus time and we obtained the pattern shown in Fig. 7. We show the calculated relation between $\Delta\alpha$ and β_1 with circles and the approximated relation with asterisks. We can see that they are practically the same, thus we can use $\Delta\alpha=(1-\beta_1)/3$ instead of the calculated relation (Eq. 8). The fact we want to remark is that this curve qualitatively reproduces the situation we have shown in Fig. 6, and if we write it in the form $\beta_1=1-3\Delta\alpha$ we can plot β_1 versus time and we can qualitatively reproduce the β_1 exponent dynamics we have shown in Fig. 3. The relation between the exponent β_1 and the width of the multifractal spectrum was obtained only in an empirical way, nevertheless, it could be interesting to establish by other ways if it can be a valid relation between these quantities.

Recently, a very interesting approach to characterize fractal time series was proposed by Kapiris et al. (2004). Their
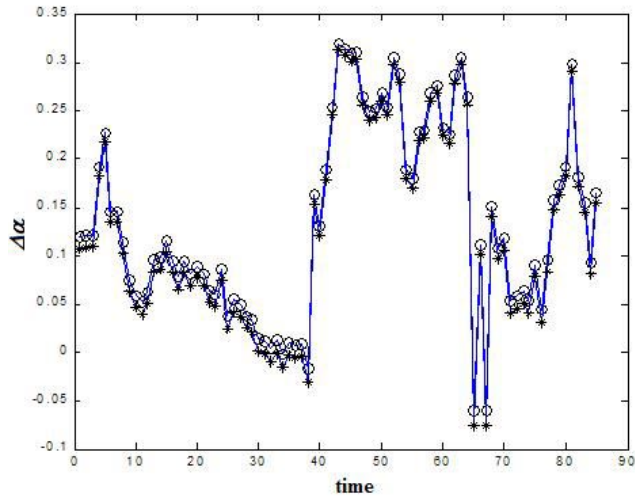
Fig. 7. $\Delta\alpha$ versus time. Calculated (circles) and approximated (asterisks). Both of them reproduce in good agreement the pattern showed in Fig. 6. Evidently the points where $\Delta\alpha < 0$ have not physical meaning. However, only around of five points are in this case.

proposal is based in the analysis of the time evolution behavior of the correlation coefficient r for VHF and UHF electroseismic signals. In this work we also study the r behavior of our ULF signals. The time evolution of the anticorrelation between $\log S(f)$ and $\log f$ is depicted in Fig. 8. It is very interesting to remark the extraordinary similarity between Fig. 7 ($\Delta\alpha$ vs. time) and Fig. 8 (r vs. time). A possible interpretation of this similarity could be related with the fact that $\Delta\alpha$ measures the complexity of the signal in the sense that we need more fractal dimensions to describe the multifractal structure if we have a high signal's variability, which corresponds with a low correlation coefficient and viceversa.

4   Concluding remarks

Within the general context of the searching for electromagnetic seismic precursors, in recent years many efforts have been made for analyzing electromagnetic data by means of methods arisen from nonlinear dynamics and statistical physics. In the present work we have used three methods (spectral analysis, DFA, and multifractal analysis) to study electroseismic time series measured in an electroseismic station located at the South Mexican Pacific coast near the trench between the North-American and Cocos tectonic plates. This is a very active seismic zone. The studied time series was collected during four months before and one month after an M_w=6.5 EQ occurred on 24 October 1993, with an epicenter 100 km distant from the station.

We first calculate the spectral exponent, and find that most of our studied files have a crossover behavior in this exponent. For low frequencies, we identify a behavior of FGN-type with β_1 within the interval (0.55, 1) in most of the cases, and a few cases with β_1 in the interval (1, 1.7) (see Fig. 3). For high frequencies $\beta_2 \approx 0$, that is, with white noise-type be-
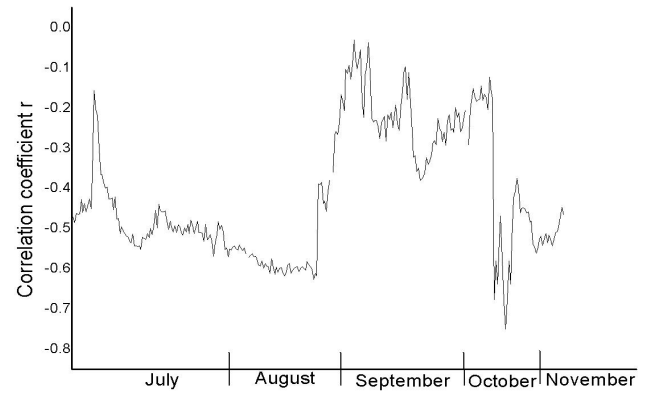

Fig. 8. Time evolution of the correlation coefficient r. Note the great similarity with Fig. 7, the r-values were calculated according to Mandel (1984).

havior. By means of the DFA method, we find (with very few exceptions) that β_1 values correspond to a time series with a persistent behavior. This fact can be the signature of an impeding instability of the considered system. Our approach for studying the electric time series is somewhat different to that employed by other authors (Varotsos et al., 2002, 2003a, b; Kapiris et al., 2004). We do not look for individual SES in the sense of Varotsos et al. (2002), but we make a global analysis of our whole time series. Thus the property of persistence exhibited by our data corresponds to the global series.

The third method was a multifractal analysis for calculating the width of the multifractal spectra $\Delta\alpha(t)$ along the five months interval. The time evolution of $\Delta\alpha$ showed an anticorrelated pattern with $\beta_1(t)$. This fact permitted to propose a simple relationship between β_1 and $\Delta\alpha$ given by Eq. (9). However, this expression needs further empirical and formal proofs. As a complementary analysis we also calculate the time evolution of the correlation coefficient r finding that it behaves in a very similar way that $\Delta\alpha(t)$.

In summary, the present paper adds some empirical results about the possible links between the behavior of electroseismic time series and impending earthquakes.

References

Balafas, J. S. and Dewey, T. G.: Multifractal analysis of solvent accessibilities in proteins, Phys. Rev. E, 52, 1, 880–887, 1995.

Chhabra, A. and Jensen, R. V.: Direct determination of the $f(\alpha)$ singularity spectrum, Phys. Rev. Lett., 62, 12, 1327–1330, 1989.

Chhabra, A., Menevau, C., Jensen, R. V., and Sreenivasan, K. R.: Direct determination of the $f(\alpha)$ singularity spectrum and its application to fully developed turbulence, Phys. Rev. A, 40, 5284–5294, 1989.

Feder, J.: Fractals, Plenum Press, New York. 1988.

Gotoh, K., Hayakawa, M., and Smirnova, N.: Fractal analysis of the ULF geomagnetic data obtained at Izu Peninsula, Japan in

relation to the nearby earthquake swarm of June–August 2000, Nat. Haz. Earth. Sys. Sci., 3, 229–236, 2003, **SRef-ID: 1684-9981/nhess/2003-3-229**.

Ivanov, P. C., Nunez Amaral, L., Goldberger, A. L., Havlin, S., Rosenblum, M. G., Struzik, Z. R., and Stanley, H. E.: Multifractality in human heartbeat dynamics, Nature, 399, 461–465, 1999.

Hayakawa, M., Ito, T., and Smirnova, N.: Fractal analysis of ULF geomagnetic data associated with the Guam earthquake on 8 August 1993, Geophys Res. Lett., 26, 2797–2800, 1999.

Hayakawa, M. and Ito, T.: ULF electromagnetic precursors for an earthquake at Biak, Indonesia on 17 February 1996, Geophys Res. Lett., 27, 1531–1534, 2000.

Heneghan, C. and McDarby, G.: Establishing the relation between detrended fluctuation analysis and power spectrum density analysis for stochastic processes, Phys. Rev. E, 62, 6103–6110, 2000.

Kapiris, P. G., Eftaxias, K. A., and Nomikos, K.: Evolving towards a critical point: A possible electromagnetic way in which the critical regime is reached as the rupture approaches, Nonl. Proc. Geophys., 10, 511–524, 2003, **SRef-ID: 1607-7946/npg/2003-10-511**.

Kapiris, P. G., Eftaxias, K. A., and Chelidze, T. L.: Electromagnetic signature of prefracture critically in heterogeneous media, Phys. Rev. Lett., 92, 065702, 2004.

Mandel, J.: The statistical analysis of experimental data, Dover Publications, Inc, New York, 1984.

Malamud, B. D. and Turcotte D. L.: Self-Affine Time Series: I Generation and Analyses, Sixth Workshop on Non-Linear Dynamics and Earthquake Prediction, H4.SMR/1330-22, 2001.

Peng, C.-K., Buldyrev, S. V., Havlin, S., Simons, M., Stanley, H. E., and Goldberger, A. L.: Mosaic organization of DNA nucleotides, Phys Rev. E, 49, 1685–1689, 1994.

Ramírez-Rojas, A., Pavía-Miller, C. G., and Angulo-Brown, F.: Statistical behavior of the spectral exponent and the correlation time of electric self-potential time series associated to the M_s=7.4 14 September 1995 earthquake in Mexico, Phys. Chem. Earth, 29, 4–9, 305–312, 2004.

Turcotte, D. L.: Fractals and Chaos in Geology and Geophysics, Cambridge University Press, 221, 1992.

Telesca, L., Cuomo, V., Lapenna, V., and Macchiato, M.: A new approach to investigate the correlation between geoelectrical time fluctuations and earthquakes in a seismic area of southern Italy, Geophys. Res. Lett., 28, 4375–4378, 2001.

Varotsos, P. A., Sarlis, N. V., and Skordas, E. S.: Long-range correlations in the electric signals that precede rupture, Phys. Rev. E, 66, 011902, 2002.

Varotsos, P. A., Sarlis, N. V., and Skordas, E. S.: Long-range correlations in the electric signals that precede rupture: Further investigations, Phys. Rev. E, 67, 021109, 2003a.

Varotsos, P. A., Sarlis, N. V., and Skordas, E. S.: Attempt to distinguish electric signals of a dichotomous nature, Phys. Rev. E, 68, 031106, 2003b.

Yépez, E., Angulo-Brown, F., Peralta, J. A., Pavía-Miller, C. G., and González-Santos, G.: Electric fields patterns as seismic precursors, Geophys. Res. Lett. 22, 3087–3090. 1995.

Yamasaki, K. and Mackin, K. J.: Market simulation displaying multifractality, e-print, cond-mat/0304331, 2003.